NASA Contractor Report 181995
ICASE Report No. 90-13

AD-A219 518

ICASE

HIGH ORDER ESSENTIALLY NON-OSCILLATORY SCHEMES FOR HAMILTON-JACOBI EQUATIONS

Stanley Osher
Chi-Wang Shu

DTIC
S ELECTE
MAR 1 9 1990
D

NASA
National Aeronautics and
Space Administration

Langley Research Center
Hampton, Virginia 23665-5225

90 03 19 017

HIGH ORDER ESSENTIALLY NON-OSCILLATORY SCHEMES FOR HAMILTON-JACOBI EQUATIONS[1]

Stanley Osher

Department of Mathematics, University of California

Los Angeles, CA 90024

and

Chi-Wang Shu

Division of Applied Mathematics

Brown University

Providence, RI 02912

ABSTRACT

Hamilton-Jacobi (H-J) equations are frequently encountered in applications, e.g. in control theory and differential games. H-J equations are closely related to hyperbolic conservation laws — in one space dimension the former is simply the integrated version of the latter. Similarity also exists for the multi-dimensional case, and this is helpful in the design of difference approximations. In this paper we investigate high order essentially non-oscillatory (ENO) schemes for H-J equations, which yield uniform high order accuracy in smooth regions and resolve discontinuities in the derivatives sharply. The ENO scheme construction procedure is adapted from that for hyperbolic conservation laws. We numerically test the schemes on a variety of one-dimensional and two-dimensional problems, including a problem related to control-optimization, and observe high order accuracy in smooth regions, good resolution of discontinuities in the derivatives, and convergence to viscosity solutions.

1. INTRODUCTION

The Hamilton-Jacobi (H-J) equation

$$\begin{cases} \phi_t + H(\phi_{x_1}, \ldots, \phi_{x_d}) = 0 \\ \phi(x,0) = \phi_0(x) \end{cases} \tag{1.1}$$

appears often in applications, e.g., in control theory and differential games. The solutions to (1.1) typically are continuous but with discontinuous derivatives, even if the initial condition $\phi_0(x)$ is C^∞. The non-uniqueness of such solutions to (1.1) also necessitates the introduction of the notions of entropy condition and viscosity solutions, to single out a unique practically relevant solution. See, e.g. Crandall and Lions [1] for details.

An important class of numerical methods for solving (1.1) is the class of monotone schemes discussed by Crandall and Lions [2]. Monotone schemes are proven convergent to the viscosity solutions. Unfortunately monotone schemes are at most first order accurate. Traditional high order methods are unsuitable, because spurious oscillations will generally occur in the presence of discontinuous derivatives.

There is a close relation between (1.1) and a hyperbolic conservation law

$$\begin{cases} u_t + \sum_{i=1}^d f_i(u)_{x_i} = 0 \\ u(x,0) = u_0(x). \end{cases} \tag{1.2}$$

In fact, for the one dimensional case $d = 1$, (1.1) is equivalent to (1.2) if we take $u = \phi_x$. For multi-dimensions this direct correspondence disappears, but in some sense we can still think about (1.1) as (1.2) "integrated once". Hence successful numerical methodology for solving hyperbolic conservation laws (1.2) should also be applicable to the H-J equation (1.1).

Essentially non-oscillating (ENO) schemes have been very successful in solving the hyperbolic conservation law (1.2), Harten and Osher [3], Harten, Engquist, Osher and Chakravarthy [4], Shu and Osher [7], [8]. The key idea is an adaptive stencil interpolation which automatically obtains information from the locally smoothest region, hence yields a uniformly high order essentially non-oscillatory approximation for piecewise smooth functions. We summarize this ENO interpolation procedure as follows:

Given point values $f(x_j), j = 0, \pm 1, \pm 2, \ldots$ of a (usually piecewise smooth) functions at discrete nodes x_j, we associate a r-th degree polynomial $P_{j+1/2}^{f,r}(x)$ with each interval $[x_j, x_{j+1}]$, constructed inductively as follows:

(1) $\quad P_{j+1/2}^{f,1}(x) = f[x_j] + f[x_j, x_{j+1}](x - x_j), \quad k_{\min} = j$

$$(1.3)$$

(2) $\quad$ If $k_{\min}^{(\ell-1)}$ and $P_{j+1/2}^{f,\ell-1}(x)$ are both defined, then let

$$a^{(\ell)} = f[x_{k_{\min}^{(\ell-1)}}, \ldots, x_{k_{\min}^{(\ell-1)}+\ell}]$$
$$b^{(\ell)} = f[x_{k_{\min}^{(\ell-1)}-1}, \ldots, x_{k_{\min}^{(\ell-1)}+\ell-1}]$$

and

(i) $\quad$ if $\quad |a^{(\ell)}| \geq |b^{(\ell)}|$, then $c^{(\ell)} = b^{(\ell)}$, $k_{\min}^{(\ell)} = k_{\min}^{(\ell-1)} - 1$

$\qquad\qquad$ otherwise $c^{(\ell)} = a^{(\ell)}$, $k_{\min}^{(\ell)} = k_{\min}^{(\ell-1)}$

(ii) $\quad\quad\quad\quad P_{j+1/2}^{f,\ell}(x) = P_{j+1/2}^{f,\ell-1}(x) + c^{(\ell)} \prod_{i=k_{\min}^{(\ell-1)}}^{k_{\min}^{(\ell-1)}+\ell-1} (x - x_i)$

$\square$

2

In the above procedure $f[\cdot, \ldots, \cdot]$ are the usual Newton divided differences. Notice that we can also start from one node x_j to build a polynomial $P_j^{f,r}(x)$ using the same procedure.

In [6] Osher and Sethian constructed ENO type schemes and applied them to a class of H-J equations and perturbations, arising in front propagation problems. They achieved very good numerical results. In this paper we provide a more general ENO scheme construction procedure, mainly by considering different multidimensional monotone building blocks. We then numerically test the schemes on a variety of one and two dimensional problems including a problem related to control-optimization, check the accuracy in smooth regions, the resolution of discontinuities in derivatives, and the phenomenon of convergence to viscosity solutions. Concluding remarks are given in Section 4.

2. SCHEME CONSTRUCTION

For simplicity of exposition we take $d = 2$ in (1.1), and use x, y instead of x_1, x_2:

$$\begin{cases} \phi_t + H(\phi_x, \phi_y) = 0 \\ \phi(x, y, 0) = \phi_0(x, y) \end{cases} \tag{2.1}$$

For mesh sizes $\Delta x, \Delta y, \Delta t, \phi_{ij}^n$ will denote a numerical approximation to the viscosity solution $\phi(x_i, y_j, t^n) = \phi(i\Delta x, j\Delta y, n\Delta t)$ of (2.1). We also use standard notation such as

$$\lambda_x = \frac{\Delta t}{\Delta x}, \lambda_y = \frac{\Delta t}{\Delta y}, \Delta_{\pm}^x \phi_{ij} = \pm(\phi_{i\pm1,j} - \phi_{ij}), \Delta_{\pm}^y \phi_{ij} = \pm(\phi_{i,j\pm1} - \phi_{ij})$$

We start with a first order monotone scheme [2]:

$$\phi_{ij}^{n+1} = \phi_{ij}^n - \Delta t \hat{H}\left(\frac{\Delta_+^x \phi_{ij}^n}{\Delta x}, \frac{\Delta_-^x \phi_{ij}^n}{\Delta x}, \frac{\Delta_+^y \phi_{ij}^n}{\Delta y}, \frac{\Delta_-^y \phi_{ij}^n}{\Delta y}\right) \tag{2.2}$$

3

where $\hat{H}$ is a Lipschitz continuous monotone flux consistent with H:

$$\hat{H}(u, u, v, v) = H(u, v).$$

Monotonicity here means that $\hat{H}$ is non-increasing in its first and third arguments and non-decreasing in the other two. Symbolically $H(\downarrow, \uparrow, \downarrow, \uparrow)$.

We now give some examples of monotone fluxes $\hat{H}$:

(1) Lax-Friedrichs [2]:

$$\hat{H}^{LF}(u^+, u^-, v^+, v^-) = H\left(\frac{u^+ + u^-}{2}, \frac{v^+ + v^-}{2}\right) - \frac{1}{2}\alpha^x(u^+ - u^-) - \frac{1}{2}\alpha^y(v^+ - v^-) \quad (2.3)$$

where

$$\alpha^x = \max_{\substack{A \leq u \leq B \\ C \leq v \leq D}} |H_1(u, v)|, \qquad \alpha^y = \max_{\substack{A \leq u \leq B \\ C \leq v \leq D}} |H_2(u, v)| \quad (2.4)$$

Here $H_i(u, v)$ is the partial derivative of H with respect to the ith argument. The flux $\hat{H}^{LF}$ is monotone for $A \leq u^\pm \leq B$, $C \leq v^\pm \leq D$;

(2) Godunov type [5]:

$$\hat{H}^G(u^+, u^-, v^+, v^-) = \operatorname*{ext}_{u \in I(u^-, u^+)} \operatorname*{ext}_{v \in I(v^-, v^+)} H(u, v) \quad (2.5)$$

where

$$I(a, b) = [\min(a, b), \ \max(a, b)]$$

and the function ext is defined by

$$\operatorname*{ext}_{u \in I(a,b)} = \begin{cases} \min_{a \leq u \leq b} & \text{if} \quad a \leq b \\ \max_{b \leq u \leq a} & \text{if} \quad a > b \end{cases} \quad (2.7)$$

4

As pointed out in [5], since in general $\min_u \max_v H(u,v) \neq \max_v \min_u H(u,v)$, we will generally obtain different versions of Godunov type fluxes $\hat{H}^G$, by changing the order of min and max. Uniqueness of $\hat{H}^G$ happens when, e.g., $H(u,v) = H^1(u) + H^2(v)$, and in many other cases. Then, by [5], $-t\hat{H}^G(u,v)$ is the exact solution to the Riemann problem of (2.1), i.e., this is the viscosity solution of (2.1) for

$$\phi_0(x,y) = xu_0(x) + yv_0(y), \quad u_0(x) = \begin{cases} u^+, x \geq 0 \\ u^-, x < 0, \end{cases} \quad v_0(y) = \begin{cases} v^+, y \geq 0 \\ v^-, y < 0 \end{cases} \tag{2.8}$$

evaluated at $(x,y) = (0,0)$, and $t > 0$.

For this reason all monotone fluxes can be regarded as approximate Riemann solvers in this sense.

(3) Local Lax-Friedrichs (LLF) [8]:

$$\hat{H}^{LLF}(u^+,u^-,v^+,v^-) = H(\tfrac{u^++u^-}{2}, \tfrac{v^++v^-}{2}) - \tfrac{1}{2}\alpha^x(u^+,u^-)(u^+,u^-) - \tfrac{1}{2}\alpha^y(v^+,v^-)(v^+-v^-)$$

$$\tag{2.9}$$

where

$$\alpha^x(u^+,u^-) = \max_{\substack{u \in I(u^-,u^+) \\ C \leq v \leq D}} |H_1(u,v)|, \quad \alpha^y(v^+,v^-) = \max_{\substack{v \in I(v^-,v^+) \\ A \leq u \leq B}} |H_2(u,v)| \tag{2.10}$$

In the appendix we prove that $\hat{H}^{LLF}$ is monotone for $A \leq u^\pm \leq B$, $C \leq v^\pm \leq D$; Notice that $\hat{H}^{LLF}$ has smaller dissipation than $\hat{H}^{LF}$.

(4) Roe with LLF entopy correction [8]:

$$\hat{H}^{RF}(u^+,u^-,v^+,v^-) = \begin{cases} H(u^*,v^*); & \text{if } H_1(u,v) \text{ and } H_2(u,v) \text{ do not change signs} \\ & \quad \text{in } u \in I(u^-,u^+), \ v \in I(v^-,v^+); \\ H(\frac{u^++u^-}{2},v^*) - \frac{1}{2}\alpha^x(u^+,u^-)(u^+ - u^-); & \text{otherwise and if } H_2(u,v) \\ & \quad \text{does not change sign in } A \le u \le B, v \in I(v^-,v^+) \\ H(u^*,\frac{v^++v^-}{2}) - \frac{1}{2}\alpha^y(v^+,v^-)(v^+ - v^-); & \text{otherwise and if } H_1(u,v) \\ & \quad \text{does not change sign in } u \in I(u^-,u^+), C \le v \le D, \\ \hat{H}^{LLF}(u^+,u^-,v^+,v^-); & \text{otherwise} \end{cases}$$

$$(2.11)$$

where u^*, v^* are defined by upwinding:

$$u^* = \begin{cases} u^+ & \text{if } H_1(u,v) \le 0 \\ u^- & \text{if } H_1(u,v) \ge 0 \end{cases}; \quad v^* = \begin{cases} v^+ & \text{if } H_2(u,v) \le 0 \\ v^- & \text{if } H_2(u,v) \ge 0 \end{cases}. \quad (2.12)$$

We will prove in the appendix that $\hat{H}^{RF}$ is monotone for $A \le u^\pm \le B$, $C \le v^\pm \le D$. Notice that $\hat{H}^{RF}$ is simple to code, purely upwinding, with almost as small dissipation as $\hat{H}^G$. Also notice that $\hat{H}^{RF}$ is not continuous: for example if $H(u) = \frac{u^2}{2}$ (one space dimension) then $\hat{H}^{RF}(1,0) = 0$ but $\hat{H}^{RF}(1,-\varepsilon) = \frac{(\frac{1-\varepsilon}{2})^2}{2} - \frac{1}{2} \cdot 1 \cdot (1+\varepsilon) \xrightarrow{\varepsilon \to 0^+} -\frac{3}{8} \ne 0$. However, this type of discontinuity does not hurt, because we have

$$|\hat{H}^{RF}(u^+,u^-,v^+,v^-) - \hat{H}^G(u^+,u^-,v^+,v^-)| \le M(|u^+ - u^-| + |v^+ - v^-|); \quad (2.13)$$

hence we still get consistency and accuracy.

REMARK 2.1. A flux with even smaller dissipation than $\hat{H}^{LLF}$ is

$$\hat{H}^{LLLF}(u^+,u^-,v^+,v^-) = H(\frac{u^++u^-}{2}, \frac{v^++v^-}{2}) - \frac{1}{2}\alpha^x(u^\pm,v^\pm)(u^+-u^-) - \frac{1}{2}\alpha^y(u^\pm,v^\pm)(v^+-v^-)$$

$$(2.14)$$

6

where

$$\alpha^x(u^\pm, v^\pm) = \max_{\substack{u \in I(u^-, u^+) \\ v \in I(v^-, v^+)}} |H_1(u,v)|, \quad \alpha^y(u^\pm, v^\pm) = \max_{\substack{u \in I(u^-, u^+) \\ v \in I(v^-, v^+)}} |H_2(u,v)|. \qquad (2.15)$$

Unfortunately it is not monotone: for example, if $H(u,v) = e^{u+v}$, then $\hat{H}^{LLLF}(2,0,0,20) > \hat{H}^{LLLF}(0,0,0,20)$. For separable Hamiltonians with $H(u,v) = H^1(u) + H^2(v)$ we have $\hat{H}^{LLLF} = \hat{H}^{LLF}$.

We now begin the description of our high order ENO schemes. Monotone fluxes play the role of "building blocks". The ENO interpolation idea in (1.3) is used to obtain high order non-oscillatory approximations to $u^\pm = \phi_x^\pm$ and $v^\pm = \phi_y^\pm$. These values are then put into a monotone flux $\hat{H}(u^+, u^-, v^+, v^-)$. Time accuracy is obtained by a class of TVD Runge-Kutta type time discretizations [7]. We summarize the algorithm as follows:

ALGORITHM 2.1:

(1) At any node (i,j), fix j to compute along the x-direction, by using (1.3), obtaining

$$u_{ij}^\pm = \tfrac{d}{dx} P_{i\pm\frac{1}{2},j}^{\phi,r}(x_i). \qquad (2.16)$$

Similarly for $v_{ij}^\pm$. Then let

$$L_{ij} = -\Delta t \hat{H}(u_{ij}^+, u_{ij}^-, v_{ij}^+, v_{ij}^-) \qquad (2.17)$$

(2) obtain ϕ^{n+1} from ϕ^n by the following Runge-Kutta type procedure:

$$\phi_{ij}^{(k)} = \sum_{\ell=0}^{k-1} [\alpha_{k\ell} \phi_{ij}^{(\ell)} + \beta_{k\ell} L_{ij}^{(\ell)}] \qquad k = 1, \ldots, \bar{r} \qquad (2.18a)$$

7

$$\phi_{ij}^{(0)} = \phi_{ij}^{n}, \quad \phi_{ij}^{(\bar{r})} = \phi_{ij}^{n+1} \tag{2.18b}$$

$\square$

We can take $\bar{r} = r$ and positive $\alpha_{k\ell}$ and $\beta_{k\ell}$ for up to third order $r \leq 3$. The method (2.18) can be proven TVD under the CFL condition:

$$\lambda = \frac{\Delta t}{\Delta x} \leq C_r \lambda_0 \tag{2.19}$$

if the Euler forward version of (2.17) is TVD under the CFL condition

$$\lambda = \frac{\Delta t}{\Delta x} \leq \lambda_0. \tag{2.20}$$

We summarize some of the schemes (2.18) in Table 2.1:

Table 2.1 TVD Runge-Kutta method (2.19)

Order	$\alpha_{k\ell}$				$\beta_{k\ell}$				C_r
2	1				1				1
	$\frac{1}{2}$	$\frac{1}{2}$			0	$\frac{1}{2}$			
3	1				1				1
	$\frac{3}{4}$	$\frac{1}{4}$			0	$\frac{1}{4}$			
	$\frac{1}{3}$	0	$\frac{2}{3}$		0	0	$\frac{2}{3}$		
4	1				$\frac{1}{2}$				$\frac{2}{3}$
	$\frac{1}{2}$	$\frac{1}{2}$			$-\frac{1}{4}$	$\frac{1}{2}$			
	$\frac{1}{9}$	$\frac{2}{9}$	$\frac{2}{3}$		$-\frac{1}{9}$	$-\frac{1}{3}$	1		
	0	$\frac{1}{3}$	$\frac{1}{3}$	$\frac{1}{3}$	0	$\frac{1}{6}$	0	$\frac{1}{6}$	

Algorithm 2.1 is formally uniformly r-th order in space and time in smooth regions (measured by local truncation errors).

Notice that in the algorithm above, we need to evaluate two polynomials $P^{\phi,r}_{i\pm\frac{1}{2},j}$ to get $u^{\pm}$. If the monotone flux is purely upwind and there is no "sonic point" (points at which H_1 or H_2 changes sign), one of u^+ and u^- is never used. We thus recommend the following:

ALGORITHM 2.2:

(1) Compute $\tilde{u}^{\pm}_{ij} = \frac{\Delta^x_{\pm}\phi^n_{ij}}{\Delta x}$ and $\tilde{v}^{\pm}_{ij} = \frac{\Delta^y_{\pm}\phi^n_{ij}}{\Delta y}$. If $H_1(u,v)$ and $H_2(u,v)$ do not change signs in $u \in I(\tilde{u}^-_{ij}, \tilde{u}^+_{ij})$, $v \in I(\tilde{v}^-_{ij}, \tilde{v}^+_{ij})$, then compute only u^*_{ij} and v^*_{ij} by (2.16) where u^*, v^* are defined by (2.12); and take $L_{ij} = -\Delta t H(u^*, v^*)$; otherwise take (2.17).

(2) Same as step (2) in Algorithm 2.1. $\qquad\qquad\square$

Notice that Algorithm 2.2 is NOT equivalent to Algorithm 2.1 with $\hat{H} = \hat{H}^{RF}$. Since we expect sonic points to be isolated, Algorithm 2.2 is usually almost twice as fast as Algorithm 2.1.

REMARK 2.2. Notice that, in smooth regions, by Taylor expansion,

$$\frac{d}{dx}P^{\phi,r}_{i\pm\frac{1}{2}}(x_i) - \frac{\Delta_{\pm}\phi_i}{\Delta x} = \frac{\Delta x}{2}\phi_{xx}(\xi). \tag{2.21}$$

If we choose, instead of (2.16),

$$u^{\pm}_{ij} = \mathbf{P}_{[\frac{\Delta^x_{\pm}\phi_{ij}}{\Delta x}, M\Delta x]}\left(\frac{d}{dx}P^{\phi,r}_{i\pm\frac{1}{2},j}(x_i)\right) \tag{2.22}$$

where the projection $\mathbf{P}$ is defined by

$$\mathbf{P}_{[a,b]}(y) = \begin{cases} y, & \text{if } a - b \leq y \leq a + b \\ a - b, & \text{if } y < a - b \\ a + b, & \text{if } y > a + b \end{cases} \tag{2.23}$$

9

we will still have uniform high order accuracy $u_{ij}^{\pm} = (\phi_x)_{ij} + O(\Delta x^r)$ in any region where $|\phi_{xx}| \leq 2M$. Algorithm 2.1 will then give a scheme which deviates from a monotone scheme by $M\Delta t \Delta x$, hence we trivially obtain convergence to the viscosity solution through the theory for monotone schemes. In practice we do not recommend (2.22), because the parameter M is not intrinsic – it has to be adjusted for each individual problem. See [7, p. 452] for a discussion of a similar situation for conservation laws.

REMARK 2.3. When implementing (1.3) we use undivided differences:

$$\varphi(j,0) = \varphi_j \tag{2.24a}$$

$$\varphi(j,k) = \varphi(j+1,k-1) - \varphi(j,k-1), \quad k = 1,\dots,r+1 \tag{2.24b}$$

The computation of (2.24) can be easily vectorized. The ENO stencil-choosing process is, for computing $u^+ = (\varphi_x)^+$, starting with $i(j) = j$ and performing

$$\text{if } (\text{abs}(\varphi(i(j),k)). \text{ gt. abs}(\varphi(i(j)-1,k))) \quad i(j) = i(j) - 1 \tag{2.25}$$

for $k = 2,\dots,r$, where $i(j)$ is the left-most point in the stencil for $P_{j+\frac{1}{2}}^{\varphi,r}(x)$. This can also be vectorized. Finally

$$u_j^+ = (\varphi_x)_j^+ = \frac{1}{\Delta x} \sum_{k=1}^{r} c(i(j) - j, k) \varphi(i(j), k) \tag{2.26}$$

where

$$c(m,k) = \frac{1}{k!} \sum_{s=m}^{m+k-1} \prod_{\substack{\ell=m \\ \ell \neq s}}^{m+k-1} (-\ell). \tag{2.27}$$

Notice that the small matrix c is independent of φ, is only computed once and then stored. (2.26) can be vectorized easily as well.

3. NUMERICAL RESULTS

EXAMPLE 1. One dimension. We solve

$$\begin{cases} \phi_t + H(\phi_x) = 0 \\ \phi(x,0) = -\cos \pi x \end{cases} \qquad -1 \le x < 1 \qquad (3.1)$$

with a convex H (Burgers' equation):

$$H(u) = \frac{(u + \alpha)^2}{2} \qquad (3.2)$$

and a non-convex H:

$$H(u) = -\cos(u + \alpha). \qquad (3.3)$$

Notice that if we let $v = \phi_x + \alpha$, $f(v) = H(v - \alpha)$, then (3.1) becomes a conservation law

$$\begin{cases} v_t + f(v)_x = 0 \\ v(x,0) = \alpha + \pi \sin \pi x \end{cases} \qquad -1 \le x < 1 \qquad (3.4)$$

which is a standard test problem for conservation laws (e.g. [7]). We can easily use the method of characteristics to obtain the exact solution of (3.1) through that of (3.4).

We take $\alpha = 1$ and compute the result to $t = t_1 = \frac{0.5}{\pi^2}$ (when the solution is still smooth) and to $t = t_2 = \frac{1.5}{\pi^2}$ (when the solution has a discontinuous derivative). We print out the L_1 and L_∞ errors, in Table 3.1, for selected first order monotone schemes and third order ENO schemes in smooth regions, i.e. the whole region [-1,1] for $t = t_1$ and the region $|x - x_s| \ge 0.1$ for $t = t_2$ where x_s is the location of any discontinuity of the derivative. We also present the graphs of the numerical solutions (in diamonds) versus the exact solutions (in solid lines) in Figures 1 and 2.

11

Table 3.1 L_1 and L_∞ Errors in Smooth Regions for (3.1)

Time			$t = 0.5/\pi^2$				$t = 1.5/\pi^2$			
# of pts			10	20	40	80	10	20	40	80
Burger's equation $H(u) = \frac{(u+1)^2}{2}$	LF	L_1	1.01(-1)	5.10(-2)	2.59(-2)	1.31(-2)	2.01(-1)	1.13(-1)	6.11(-2)	3.16(-2)
		L_∞	1.81(-1)	1.08(-1)	6.03(-2)	3.23(-2)	3.17(-1)	1.72(-1)	8.48(-2)	4.59(-2)
	Godunov	L_1	3.36(-2)	1.50(-2)	7.66(-3)	3.87(-3)	5.94(-2)	3.18(-2)	1.70(-2)	8.50(-3)
		L_∞	7.40(-2)	3.61(-2)	1.93(-2)	1.01(-2)	1.12(-1)	5.93(-2)	3.00(-2)	1.51(-2)
	ENO-3-LF	L_1	1.13(-2)	1.83(-3)	2.59(-4)	4.27(-5)	1.65(-2)	2.32(-3)	2.61(-4)	4.17(-5)
		L_∞	3.16(-2)	5.08(-3)	8.75(-4)	2.07(-4)	3.40(-2)	7.81(-3)	1.33(-3)	1.07(-4)
	ENO-3-God	L_1	5.74(-3)	9.55(-4)	1.41(-4)	2.56(-5)	7.37(-3)	1.18(-3)	1.46(-4)	2.85(-5)
		L_∞	1.52(-2)	4.48(-3)	7.55(-4)	1.52(-4)	2.29(-2)	6.76(-3)	9.79(-4)	1.04(-4)
	ENO-3-RF	L_1	5.79(-3)	9.56(-4)	1.42(-4)	2.56(-5)	8.19(-3)	1.15(-3)	1.46(-4)	2.85(-5)
		L_∞	1.52(-2)	4.48(-3)	7.55(-4)	1.52(-4)	2.29(-2)	5.92(-3)	9.97(-4)	1.04(-4)
Non-convex $H(u) = -\cos(u+1)$	LF	L_1	2.70(-2)	1.19(-2)	5.56(-3)	2.58(-3)	5.51(-2)	2.83(-2)	1.33(-2)	6.43(-3)
		L_∞	4.15(-2)	2.36(-2)	1.30(-2)	6.98(-3)	1.03(-1)	4.72(-2)	2.29(-2)	1.12(-2)
	Godunov	L_1	1.52(-2)	5.89(-3)	2.46(-3)	1.16(-3)	2.41(-2)	1.13(-2)	5.45(-3)	2.60(-3)
		L_∞	3.52(-2)	1.22(-2)	5.88(-3)	2.57(-3)	4.69(-2)	2.56(-2)	1.26(-2)	5.78(-3)
	ENO-3-LF	L_1	1.62(-3)	5.68(-4)	8.92(-5)	9.47(-6)	8.81(-3)	1.35(-3)	1.84(-4)	2.43(-5)
		L_∞	6.23(-3)	2.33(-3)	4.81(-4)	1.06(-4)	1.39(-2)	9.07(-3)	1.53(-3)	2.14(-4)
	ENO-3-God	L_1	1.05(-3)	3.17(-4)	5.92(-5)	7.57(-6)	7.05(-3)	9.10(-4)	1.51(-4)	2.56(-5)
		L_∞	3.13(-3)	1.17(-3)	2.66(-4)	4.39(-5)	1.31(-2)	5.93(-3)	1.39(-3)	2.01(-4)
	ENO-3-RF	L_1	1.11(-3)	3.21(-4)	5.92(-5)	7.57(-6)	6.31(-3)	9.10(-4)	1.51(-4)	2.60(-5)
		L_∞	3.44(-3)	1.17(-3)	2.66(-4)	4.39(-5)	1.27(-2)	5.94(-3)	1.39(-3)	2.01(-4)

REMARK 3.1. From Table 3.1 and Figures 1 and 2 we can observe that:

(i) the resolution of third order ENO schemes with 10 points is roughly the same as that of the corresponding monotone schemes with 80 points;

(ii) ENO-3-Godunov and ENO-3-RF have roughly the same resolution, even if the latter is much simpler than the former and only takes about half time. $\square$

EXAMPLE 2. Two dimensions. We solve

$$
\begin{cases}
\phi_t + H(\phi_x, \phi_y) = 0 \\
\phi(x, y, 0) = -\cos \pi \left(\frac{x+y}{2} \right)
\end{cases}
\quad -2 \leq x, y \leq 2
\tag{3.5}
$$

with a convex H (Burgers' equation):

$$
H(u, v) = \frac{(u + v + \alpha)^2}{2}
\tag{3.6}
$$

and a non-convex H:

$$
H(u, v) = -\cos(u + v + \alpha).
\tag{3.7}
$$

Notice that, under the transformation $\xi = \frac{x+y}{2}$, $\eta = \frac{x-y}{2}$, (3.5) - (3.6) - (3.7) become (3.1) - (3.2) - (3.3) in the ξ direction. We can thus use the one dimensional exact solution to analyze our numerical results. Since we use (x, y) coordinates, this is a true two dimensional test problem.

We again take $\alpha = 1$ and compute to $t = t_1 = \frac{0.5}{\pi^2}$ and $t = t_2 = \frac{1.5}{\pi^2}$. Some results are presented in Table 3.2 and Figure 3.

Table 3.2 L_1 and L_∞ Errors in Smooth Regions for (3.5)

Time			$t = 0.5/\pi^2$				$t = 1.5/\pi^2$			
# of points			10^2	20^2	40^2	80^2	10^2	20^2	40^2	80^2
$H = \frac{(u+v+1)^2}{2}$	LF	L_1	1.01(-1)	5.10(-2)	2.59(-2)	1.31(-2)	2.24(-1)	1.25(-1)	6.79(-2)	3.51(-2)
		L_∞	1.81(-1)	1.08(-1)	6.03(-2)	3.23(-2)	3.17(-1)	1.72(-1)	8.98(-2)	4.59(-2)
	ENO-3-LF	L_1	1.15(-2)	1.83(-3)	2.59(-4)	4.25(-5)	1.83(-2)	2.58(-3)	2.90(-4)	4.64(-5)
		L_∞	3.37(-2)	5.09(-3)	8.75(-4)	2.11(-4)	3.41(-2)	7.82(-3)	1.34(-3)	1.15(-4)
$H = -\cos(u+v+1)^2$	LF	L_1	2.70(-2)	1.19(-2)	5.56(-3)	2.58(-3)	8.01(-2)	3.56(-2)	1.67(-2)	8.03(-3)
		L_∞	4.15(-2)	2.36(-2)	1.30(-2)	6.98(-3)	1.03(-1)	4.72(-2)	2.29(-2)	1.12(-2)
	ENO-3-LF	L_1	1.65(-3)	5.68(-4)	8.93(-5)	9.23(-6)	1.03(-2)	1.69(-3)	2.20)-4)	4.93(-5)
		L_∞	6.23(-3)	2.33(-3)	4.82(-4)	1.07(-4)	1.42(-2)	9.10(-3)	1.56(-3)	6.13(-4)

REMARK 3.2

(i) By comparing Table 3.2 with Table 3.1 we can see that ENO schemes perform equally well in two dimensions;

(ii) Notice that, except for a sharper discontinuity-in-derivative resolution, we cannot see much difference between Figures 3(a), 3(c) (first order monotone schemes) and 3(b), 3(d) (third order ENO schemes). However, from Table 3.2 we can clearly see a large difference in the resolution of the solution in smooth regions. This indicates the limitations of graphical presentations;

14

(iii) In this two dimensional case, the Godunov flux is considerably more complicated to program than LF or RF, with a not-so-significant improvement in resolution for ENO-3. $\square$

EXAMPLE 3. We solve a two dimensional non-convex Riemann problem

$$\begin{cases} \phi_t + \sin(\phi_x + \phi_y) = 0 \\ \phi(x, y, 0) = \pi(|y| - |x|) \end{cases} \tag{3.8}$$

to investigate the resolutions of different building blocks, the behavior of different versions of Godunov flux (2.5); and convergence to viscosity solutions. The results are in Figure 4 and 5: From the graphs and computer outputs we can observe:

(i) ENO-3 with G1, G2 (two versions of Godunov fluxes), LF and RF as building blocks are all convergent to the viscosity solution, with a much sharper resolution for the discontinuities-in-derivative than the corresponding first order monotone schemes;

(ii) ENO-3-RF has roughly the same resolution as ENO-3-Godunov, with a much simpler program and a reduced computer cost;

(iii) The difference between two versions of Godunov fluxes is very small: the average difference at $t = 1$ is around 1000 times smaller than the L_1 errors.

(iv) ENO-3, using the Roe flux as a building block without entropy corrections, i.e., Algorithm 2.2 without using (2.17) for entropy corrections in "sonic cells", converges to an incorrect solution just as the first order Roe scheme (Figure 5). This indicates the importance of entropy corrections in "sonic cells".

EXAMPLE 4. We solve the following problem related to control–optimal cost determination:

$$\begin{cases} \phi_t - (\sin y)\phi_x + (\sin x + \text{sign}(\phi_y))\phi_y - \frac{1}{2}\sin^2 y - (1 - \cos x) = 0 \\ \phi(x, y, 0) = 0 \end{cases} \tag{3.9}$$

15

assuming periodicity. The results at $t = 1$ are presented in Figure 6. Notice that third order ENO schemes have sharper discontinuities-in-derivative resolution than first order monotone schemes. For this problem the interesting quantity is the optimal solution $w = \text{sign}(\phi_y)$, Figure 5d. A sharper discontinuities-in-derivative resolution means smaller error for w in the neighborhood of each such point.

4. CONCLUDING REMARKS

We have generalized ENO schemes for conservation laws to Hamilton-Jacobi type equations. Computational results indicate good accuracy in regions of smoothness, sharp discontinuities in derivatives, and convergence to the correct viscosity solutions. Algorithm 2.2 (ENO-RF) is usually preferred, due to its simplicity to program, reduced computational cost, and its excellent resolution, which is comparable to the results using the much more complicated Godunov type building blocks.

ACKNOWLEGEMENT

16

REFERENCES

1. M. CRANDALL and P. LIONS, Viscosity solutions of Hamilton-Jacobi equations, *Trans. Amer. Math. Soc.*, **277** (1983), 1-42.

2. M. CRANDALL and P. LIONS, Two approximations of solutions of Hamilton-Jacobi equations, *Math. Comput.*, **43** (1984), 1-19.

3. A. HARTEN and S. OSHER, Uniformly high order accurate non-oscillatory schemes, I, *Siam J. Numer. Anal.*, **24** (1987), 279-309.

4. A. HARTEN, B. ENGQUIST, S. OSHER and S. CHAKRAVARTHY, Uniformly high order accurate essentially non-oscillatory schemes, II, *J. Comput. Phys.*, **71** (1987), 231-303.

5. S. OSHER, The nonconvex multi-dimensional Riemann problem for Hamilton-Jacobi equations, *ICASE Report* 89-53 (1989).

6. S. OSHER and J. SETHIAN, Fronts propagating with curvature dependent speed: algorithms based on Hamilton-Jacobi formulations, *J. Comput. Phys.*, **79** (1988), 12-49.

7. C.-W. SHU and S. OSHER, Efficient implementation of essentially non-oscillatory shock-capturing schemes, *J. Comput. Phys.*, **77** (1988), 439-471.

8. C.-W. SHU and S. OSHER, Efficient implementation of essentially non-oscillatory shock-capturing schemes, II, *J. Comput. Phys.*, **83** (1989), 32-78.

APPENDIX

We prove that $\hat{H}^{LLF}$ and $\hat{H}^{RF}$ are both monotone. To simplify the exposition we only consider the one dimensional case. The proof for the multi dimensional case is similar.

LEMMA A.1 $\hat{H}^{LLF}$ is monotone.

Proof. $\hat{H}^{LLF}$ in one dimension is defined by

$$\hat{H}^{LLF}(u^+, u^-) = H\left(\frac{u^+ + u^-}{2}\right) - \frac{1}{2} \max_{u \in I(u^-, u^+)} |H'(u)|(u^+ - u^-). \qquad (A.1)$$

We assume $u_1^+ > u_2^+$ and want to prove $\hat{H}^{LLF}(u_1^+, u^-) \leq \hat{H}^{LLF}(u_2^+, u^-)$. Let $D = \hat{H}^{LLF}(u_1^+, u^-) - \hat{H}^{LLF}(u_2^+, u^-)$. This equals:

$$H\left(\frac{u_1^+ + u^-}{2}\right) - H\left(\frac{u_2^+ + u^-}{2}\right) - \frac{1}{2} \max_{u \in I(u^-, u_1^+)} |H'(u)|(u_1^+ - u^-) + \frac{1}{2} \max_{u \in I(u^-, u_2^+)} |H'(u)|(u_2^+ - u^-)$$

CASE (i) $u_1^+ > u_2^+ \geq u^-$. We have for $u^- \leq \frac{u_2^+ + u^-}{2} \leq \xi \leq \frac{u_1^+ + u^-}{2} \leq u_1^+$;

$$D = \frac{1}{2}\left[H'(\xi)(u_1^+ - u_2^+) - \max_{u^- \leq u \leq u_1^+} |H'(u)|(u_1^+ - u^-) + \max_{u^- \leq u \leq u_2^+} |H'(u)|(u_2^+ - u^-)\right]$$

$$\leq \frac{1}{2}\left[H'(\xi)(u_1^+ - u_2^+) - \max_{u^- \leq u \leq u_1^+} |H'(u)|(u_1^+ - u^-) + \max_{u^- \leq u \leq u_1^+} |H'(u)|(u_2^+ - u^-)\right]$$

$$= \frac{1}{2}(u_1^+ - u_2^+)\left[H'(\xi) - \max_{u^- \leq u \leq u_1^+} |H'(u)|\right] \leq 0;$$

CASE (ii) $u^- \geq u_1^+ > u_2^+$, similar to case (i);

18

CASE (iii) $u_1^+ \geq u^- \geq u_2^+$. We have, for $u^- \leq \xi \leq \frac{u_1^+ + u^-}{2} \leq u_1^+$ and $u_2^+ \leq \frac{u_2^+ + u^-}{2} \leq \eta \leq u^-$,

$$D = \frac{1}{2}\left[H'(\xi)(u_1^+ - u^-) + H'(\eta)(u^- - u_2^+) - \max_{u^- \leq u \leq u_1^+} |H'(u)|(u_1^+ - u^-) \right.$$

$$+ \max_{u_2^+ \leq u \leq u^-} |H'(u)|(u_2^+ - u^-) \Bigg]$$

$$= \frac{1}{2}(u_1^+ - u^-)\left[H'(\xi) - \max_{u^- \leq u \leq u_1^+} |H'(u)| \right] + \frac{1}{2}(u^- - u_2^+)\left[H'(\eta) - \max_{u_2^+ \leq u \leq u^-} |H'(u)| \right] \leq 0$$

Hence we proved $\hat{H}(\downarrow, \cdot)$. We can similarly prove $\hat{H}(\cdot, \uparrow)$ $\qquad \square$

LEMMA A.2 $\hat{H}^{RF}$ is monotone.

Proof. $\hat{H}^{RF}$ in one dimension is defined by

$$\hat{H}^{RF}(u^+, u^-) = \begin{cases} H(u^+) & \text{if } H'(u) \leq 0 \text{ in } u \in I(u^-, u^+) \\ H(u^-) & \text{if } H'(u) \geq 0 \text{ in } u \in I(u^-, u^+) \\ \hat{H}^{LLF}(u^+, u^-) & \text{otherwise.} \end{cases} \qquad (A.2)$$

We assume $u_1^- > u_2^-$ and want to prove $\hat{H}^{RF}(u^+, u_1^-) \geq \hat{H}^{RF}(u^+, u_2^-)$.

Let $D = \hat{H}^{RF}(u^+, u_1^-) - \hat{H}^{RF}(u^+, u_2^-)$.

CASE (i) $\hat{H}^{RF}(u^+, u_1^-) = \hat{H}^G(u^+, u_1^-)$ and $\hat{H}^{RF}(u^+, u_2^-) = \hat{H}^G(u^+, u_2^-)$ or $\hat{H}^{RF}(u^+, u^-) = \hat{H}^{LLF}(u^+, u_1^-)$ and $\hat{H}^{RF}(u^+, u_2^-) = \hat{H}^{LLF}(u^+, u_2^-)$, then automatically $D \geq 0$.

CASE (ii) $\hat{H}^{RF}(u^+, u_1^-) = H(u_1^-)$, $\hat{H}^{RF}(u^+, u_2^-) = \hat{H}^{LLF}(u^+, u_2^-)$. Then $H'(u) \geq 0$ in $I(u_1^-, u^+)$ but $H'(u)$ changes sign in $I(u_2^-, u^+)$, hence $I(u_2^-, u^+) \not\subset I(u_1^-, u^+)$. Therefore $u^+ \geq u_2^-$. We then have either

(a) $u^+ \geq u_1^- > u_2^-$, and, for $u_2^- \leq \xi \leq u^+$ we have

$$D = \frac{1}{2}\left[H'(\xi)(2u_1^- - u_2^- - u^+) + \max_{u_2^- \leq u \leq u^+} |H'(u)|(u^+ - u_2^-)\right]$$

$$= \frac{1}{2}(u^+ - u_1^-)\left[\max_{u_2^- \leq u \leq u^+} |H'(u)| - H'(\xi)\right] + \frac{1}{2}(u_1^- - u_2^-)\left[\max_{u_2^- \leq u \leq u^+} |H'(u)| + H'(\xi)\right] \geq 0$$

or (b) $u_1^- \geq u^+ \geq u_2^-$, and, since $H(u_1^-) \geq H(u^+)$ due to the fact that $H'(u) \geq 0$ in $[u^+, u_1^-]$, we have, for $u^+ \geq \xi \geq \frac{u^+ + u_2^-}{2} \geq u_2^-$,

$$D = H(u_1^-) - \hat{H}^{LLF}(u^+, u_2^-) \geq H(u^+) - \hat{H}^{LLF}(u^+, u_2^-)$$

$$= \frac{1}{2}\left[H'(\xi)(u^+ - u_2^-) + \max_{u_2^- \leq u \leq u_2^+} |H'(u)|(u^+ - u_2^-)\right]$$

$$= \frac{1}{2}(u^+ - u_2^-)\left(\max_{u_2^- \leq u \leq u^+} |H'(u)| + H'(\xi)\right) \geq 0;$$

CASE (iii) $\hat{H}^{RF}(u^+, u_1^-) = H(u^+)$, $\hat{H}^{RF}(u^+, u_2^-) = \hat{H}^{LLF}(u^+, u_2^-)$

As in case (ii) we can again deduce $u^+ \geq u_2^-$; hence, for $u_2^- \leq \frac{u^+ + u_2^-}{2} \leq \xi \leq u^+$, we have

$$D = H(u^+) - \hat{H}^{LLF}(u^+, u_2^-)$$

$$= \frac{1}{2}\left[H'(\xi)(u^+ - u_2^-) - \max_{u_2^- \leq u \leq u^+} |H'(u)|(u^+ - u_2^-)\right] \geq 0;$$

CASE (iv) $\hat{H}^{RF}(u^+, u_1^-) = \hat{H}^{LLF}(u^+, u_1^-)$, $\hat{H}^{RF}(u^+, u_2^-) = H(u_2^-)$ similar to case (ii);

CASE (v) $\hat{H}^{RF}(u^+, u^-) = \hat{H}^{LLF}(u^+, u_1^-)$, $\hat{H}^{RF}(u^+, u_2^-) = H(u^+)$ similar to case (iii).

We have proved $\hat{H}(\cdot, \uparrow)$. Similarly for $\hat{H}(\downarrow, \cdot)$ $\qquad\qquad\square$
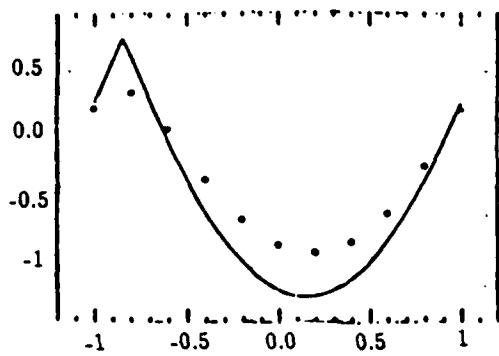
1a : First order Lax-Friedrichs, 10 points
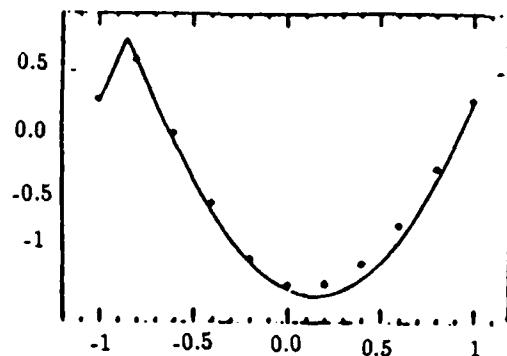
1b : First order Godunov, 10 points
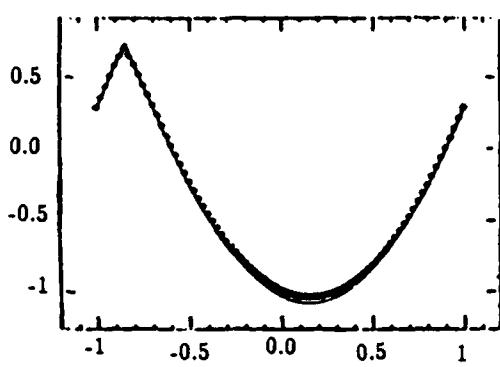
1c : First order Lax-Friedrichs, 80 points
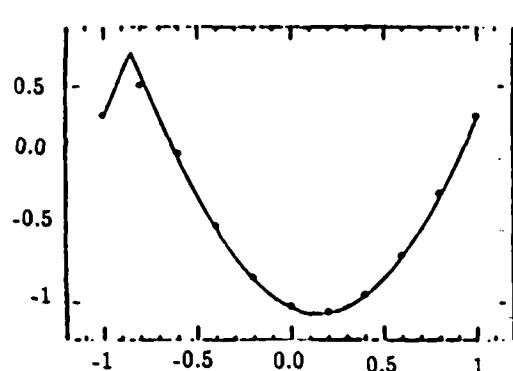
1d : Third order ENO-LF, 10 points
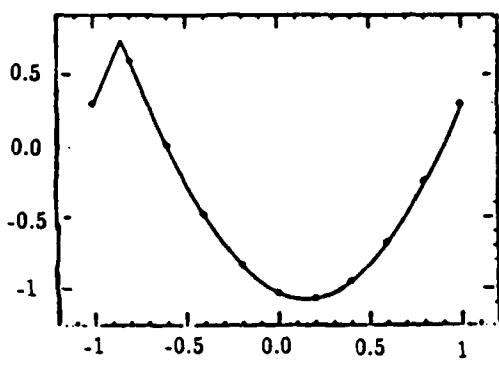
1e : Third order ENO-Godunov, 10 points
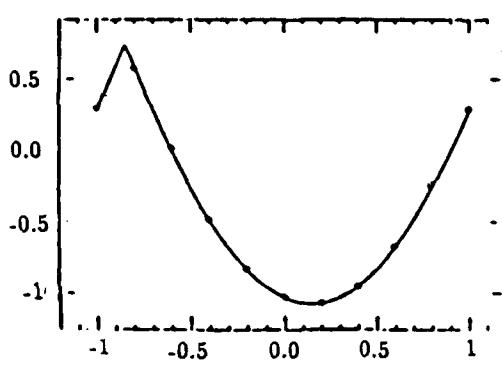
1f : Third order ENO-RF, 10 points

Figure 1 : One dimensional Burgers' equation
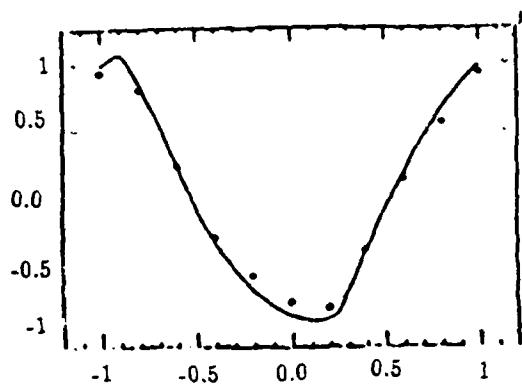
2a : First order Lax-Friedrichs, 10 points
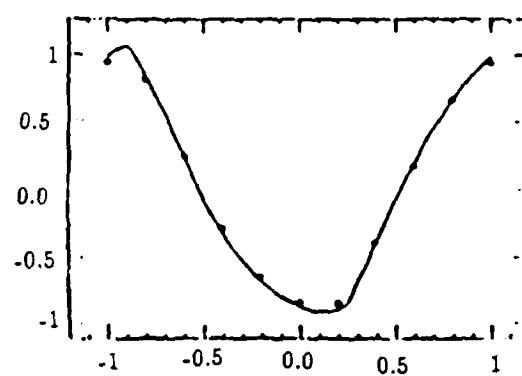
2b : First order Godunov, 10 points
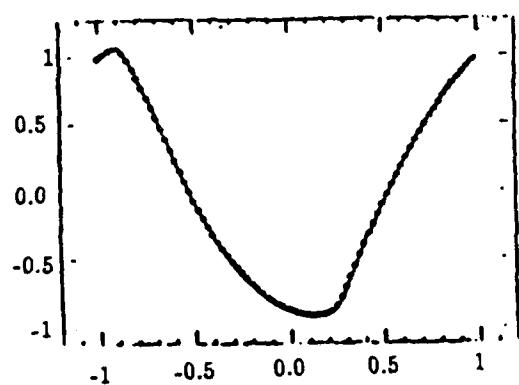
2c : First order, Lax-Friedrichs, 80 points
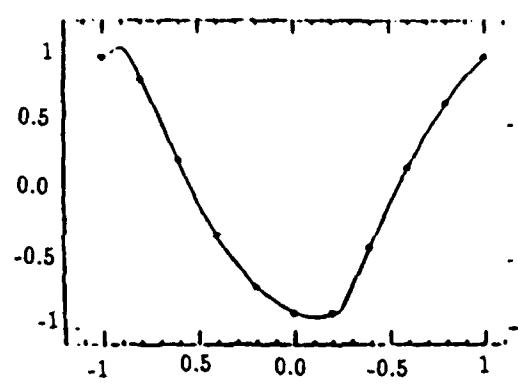
2d : Third order ENO-LF, 10 points
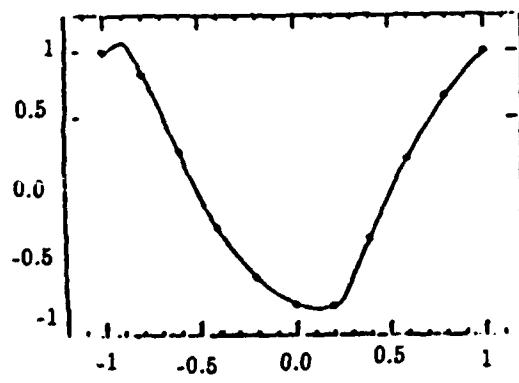
2e : Third order ENO-Godunov, 10 points
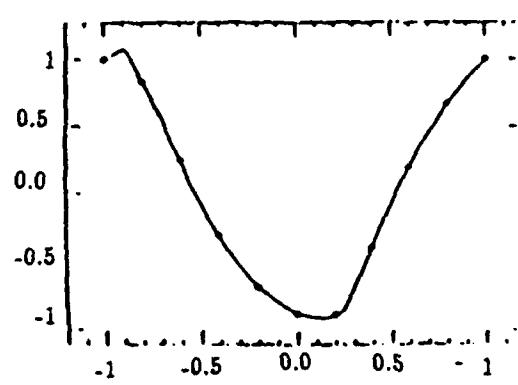
2f : Third order ENO-RF, 10 points

Figure 2: One dimension, $H(u) = -\cos(u+1)$

22
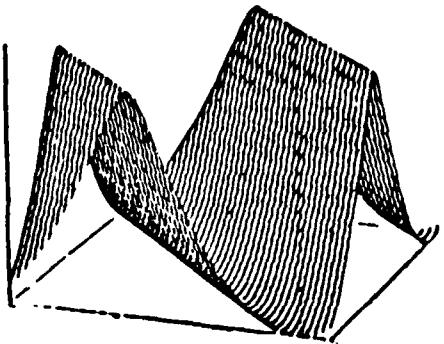
3a : First order Lax-Friedrichs, convex H
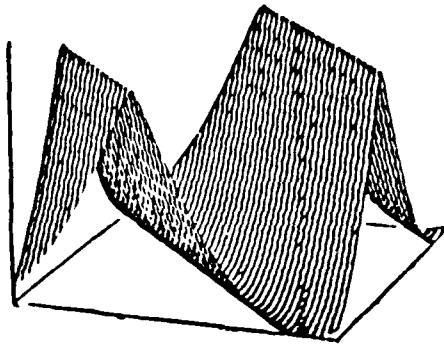
3b : ENO-3-LF, convex H
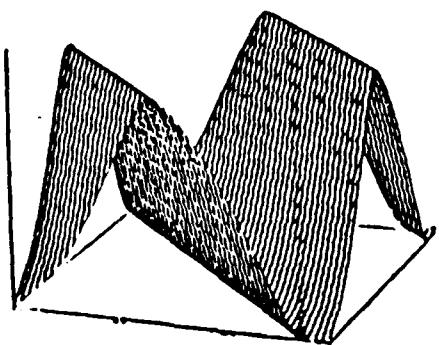
3c : First order Lax-Friedrichs, non-convex H
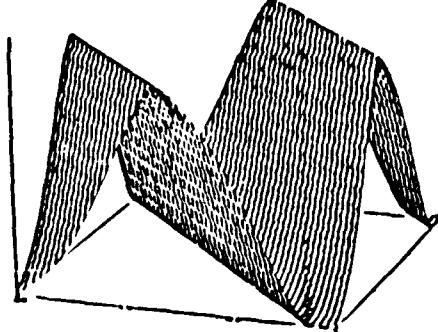
3d : ENO-3-LF, non-convex H

Figure 3: Two dimensions, 40×40 points
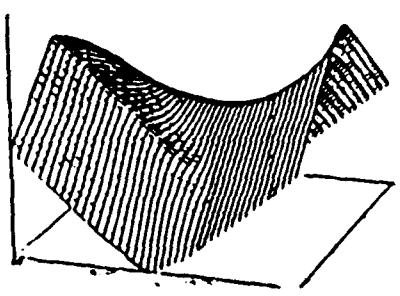
4a : First order Lax-Friedrichs
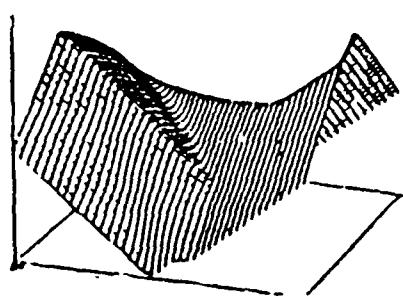
4b : ENO-3-LF
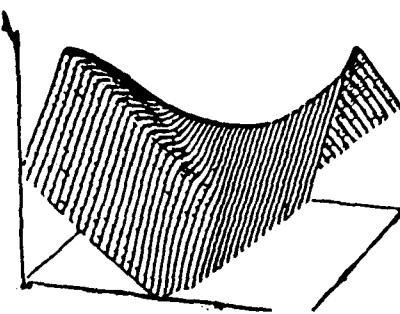
4c : First order, Godunov, version I
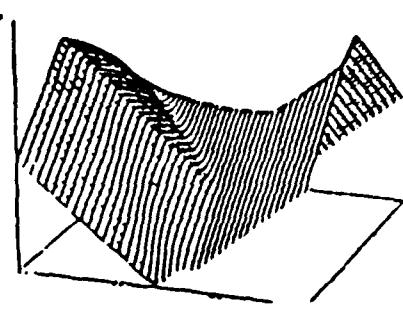
4d : ENO-3-G1
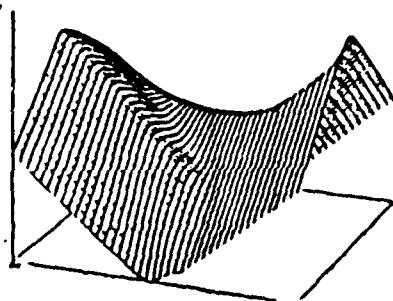
4e : First order Godunov, version II
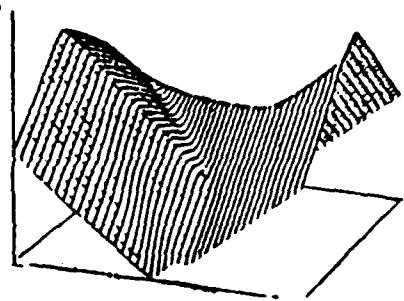
4f : ENO-3-G2
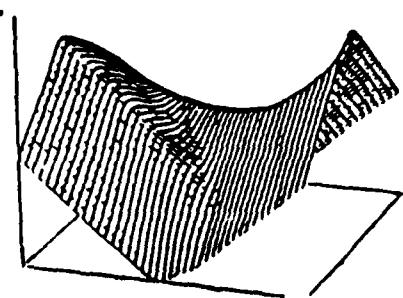
4g : First order Roe with entropy correction
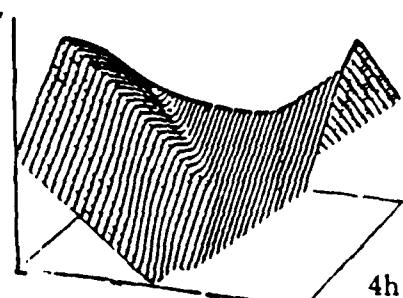
4h : ENO-3-RF

Figure 4: Riemann problem (3.8), 40×40 points, $t = 1$.
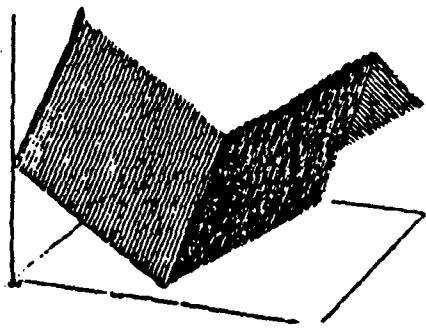
5a : First order Roe
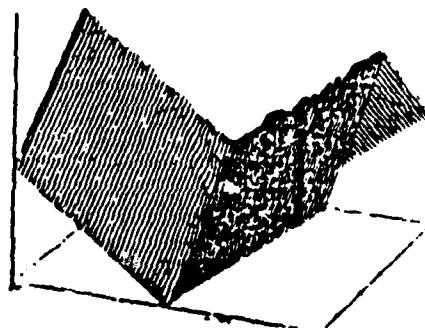
5b : ENO-3-Roe

Figure 5: Riemann problem (3.8), 80×80 points, $t = 1$
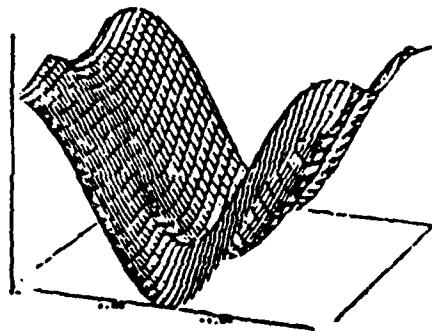
6a : First order Lax-Friedrichs
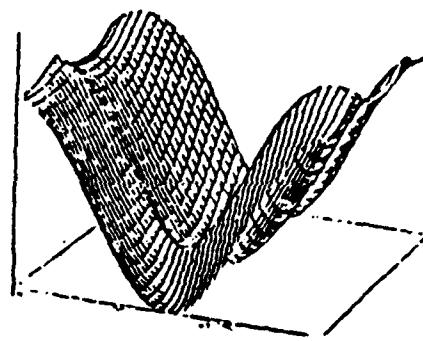
6b : ENO-3-LF
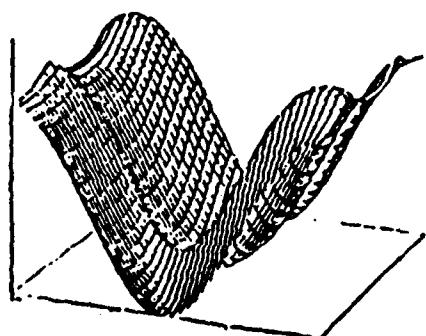
6c : ENO-3-RF
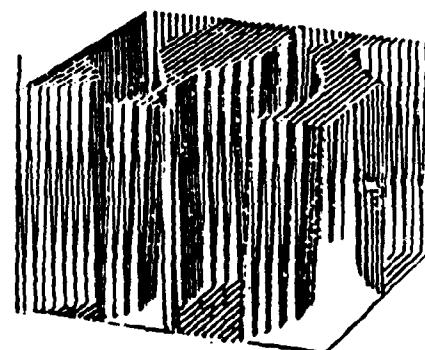
6d : $-\omega = \text{sign}(\phi_y)$, ENO-3-LF

Figure 6: Control problem (3.9), 40×40 points

25

NASA

National Aeronautics and Space Administration

Report Documentation Page

1. Report No. NASA CR-181995 ICASE Report No. 90-13	2. Government Accession No.	3. Recipient's Catalog No.
4. Title and Subtitle HIGH ORDER ESSENTIALLY NON-OSCILLATORY SCHEMES FOR HAMILTON-JACOBI EQUATIONS		5. Report Date February 1990
		6. Performing Organization Code
7. Author(s) Stanley Osher Chi-Wang Shu		8. Performing Organization Report No. 90-13
		10. Work Unit No. 505-90-21-01
9. Performing Organization Name and Address Institute for Computer Applications in Science and Engineering Mail Stop 132C, NASA Langley Research Center Hampton, VA 23665-5225		11. Contract or Grant No. NAS1-18605
		13. Type of Report and Period Covered Contractor Report
12. Sponsoring Agency Name and Address National Aeronautics and Space Administration Langley Research Center Hampton, VA 23665-5225		
		14. Sponsoring Agency Code

15. Supplementary Notes
Langley Technical Monitor: Richard W. Barnwell Final Report   Submitted to SIAM Journal of Numerical Analysis

16. Abstract

    Hamilton-Jacobi (H-J) equations are frequently encountered in application, e.g. in control theory and differential games. H-J equations are closely related to hyperbolic conservation laws - in one space dimension the former is simply the integrated version of the latter. Similarity also exists for the multi-dimensional case, and this is helpful in the design of difference approximations. In this paper we investigate high order essentially non-oscillatory (ENO) schemes for H-J equations, which yield uniform high order accuracy in smooth regions and resolve discontinuities in the derivatives sharply. The ENO scheme construction procedure is adapted from that for hyperbolic conservation laws. We numerically text the schemes on a variety of one-dimensional and two-dimensional problems, including a problem related to control-optimization, and observe high order accuracy in smooth regions, good resolution of discontinuities in the derivatives, and convergence to viscosity solutions.

17. Key Words (Suggested by Author(s))
 	
essentially non-oscillatory schemes;
  Hamilton-Jacobi equations
	18. Distribution Statement
	64 - Numerical Analysis
	59 - Mathematical and Computer
	        Sciences (General)
	
	Unclassified - Unlimited		

19. Security Classif. (of this report) Unclassified	20. Security Classif. (of this page) Unclassified	21. No. of pages 27	22. Price A03

NASA FORM 1626 OCT 86